

One-pot Synthesis of Fe₂O₃/PEDOT/rGO Nanocomposite for Sensitive Determination of Caffeine

Lei Gao¹, Ruirui Yue^{2,*}, Jingkun Xu^{1,*}, Zhen Liu¹

¹ College of Chemistry & Chemical Engineering, Jiangxi Science & Technology Normal University, Nanchang 330013, PR China

² College of Life Science, Jiangxi Science & Technology Normal University, Nanchang 330013, PR China

*E-mail: yuerui.923@163.com, yuerr@jxstnu.edu.cn, xujingkun@jxstnu.edu.cn

Received: 26 August 2017 / Accepted: 26 September 2017 / Published: 5 June 2018

In this research, a ternary nanocomposite, based on iron oxide (Fe₂O₃), reduced graphene oxide (rGO) and PEDOT had been successfully synthesized via one-pot method for the electrochemical detection of caffeine. The obtained nanocomposite Fe₂O₃/PEDOT/rGO was characterized by SEM, EDS, XRD, XPS and Raman spectroscopy to confirm the morphology, structure and composition. In addition, the electrochemical behaviors of caffeine on the nanocomposite modified electrode were investigated by cyclic voltammetry and differential pulse voltammetry. The results demonstrated that the Fe₂O₃/PEDOT/rGO nanocomposite exhibited excellent electrocatalytic activity to caffeine. Under the optimized conditions, the Fe₂O₃/PEDOT/rGO modified glassy carbon electrode showed a wide linear range of 1.0×10^{-6} to 8.0×10^{-4} M with the correlation coefficient of 0.992 and a detection limit of 3.3×10^{-7} M for the determination of caffeine. Furthermore, the modified electrode displayed high sensitivity and selectivity, good reproducibility and long-term stability in subsequent experiments. It was also successfully used to determine caffeine in beverage samples.

Keywords: Iron(III) oxide; Poly(3,4-ethylene-dioxythiophene); Graphene; Caffeine; Electrochemical sensor.

1. INTRODUCTION

Caffeine is one kind of xanthine alkaloid compounds, and it is a central nervous stimulant, can be used in the treatment of neurasthenia and coma [1]. Natural caffeine such as coffee beans, cacao beans, kola nuts, bissu nuts, guarana and tea leaves are usually added as ingredients to foods, beverages, and medications [2]. And it is widely consumed by people of all ages, especially in daily beverages, such as coffee, tea, coca-cola. According to the survey in America, most adults drink

caffeine everyday [3]. However, when it is consumed excessively, it may cause mental disorder, gastrointestinal dysfunction, and even death. Furthermore, it can cause genic mutation, such as inhibition of DNA repair, eventually lead to cancer [4]. Therefore, the accurate and quick determination of caffeine is important to food safety and people's healthy eating.

In recent years, various analytical techniques have been developed for the detection of caffeine, such as UV spectrophotometry [5], FTIR spectrophotometry [6], high-performance liquid chromatography (HPLC) [7,8], gas chromatography [9] and capillary electrophoresis [10]. However, these technologies are usually time-consuming and costly. In the determination of caffeine, electrochemical methods are more promising and desirable because of the advantages of high sensitivity, quick response, low cost and real-time analysis [11].

Owing to their excellent electrical conductivity, strong mechanical strength, high surface area, graphene (Gr) and its derivatives have attracted considerable attention in electrochemical sensor [12]. Sun et al. fabricated a Nafion-Gr modified glassy carbon electrode for the caffeine detection [13]. Zhao et al. developed a Nafion-graphene oxide modified glassy carbon electrode to determination caffeine by voltammetry [14]. However, the nafion itself has a bad electrical conductivity, and most of these binary electrode materials usually exhibit limited electrocatalytic activity towards the oxidation of caffeine [15]. In recent years, metal oxide/graphene composite materials have attracted more and more attention because of their outstanding electrochemical properties [16,17]. Radhakrishnan et al. fabricated a $\text{Fe}_2\text{O}_3/\text{rGO}$ composite for the electrochemical determination of nitrite, and the nanocomposite showed high sensing response [18]. As we all know, the electrical conductivity of metal oxide is not as good as single metal. Poly(3,4-ethylenedioxythiophene) (PEDOT), as an outstanding conducting polymer, has been widely studied owing to its high physical and chemical stability, superior conductivity, excellent compatibility and adhesion ability with other materials [19]. To improve the conductivity of metal oxide, PEDOT is undoubtedly a good choice. Accordingly, Wang et al. synthesized graphene/ SnO_2 /PEDOT ternary electrode material via one-pot method for supercapacitors [20]. Choe et al. fabricated MnO_2 /PEDOT/rGO composite by electrochemical methods for improved electrocatalytic oxygen reduction reaction [21]. To the best knowledge of the authors, there is no report about the synthesis of the Fe_2O_3 /PEDOT/rGO ternary nanocomposite or the voltammetric behaviour of caffeine at Fe_2O_3 /PEDOT/rGO modified electrodes.

In this paper, Fe_2O_3 /PEDOT/rGO ternary nanocomposite was simply fabricated by one-pot method. In addition, its electrocatalytic performance to caffeine was investigated by the cyclic voltammetry (CV) and differential pulse amperometry (DPV). As a result, the obtained Fe_2O_3 /PEDOT/rGO nanocomposite exhibited excellent electrocatalytic activity to the oxidation of caffeine.

2. EXPERIMENTAL

2.1 Apparatus

The SEM images were obtained on a Quanta-250 field emission scanning electron microscope (FEI, USA). Energy-dispersive X-ray spectroscopy (EDX) was tested by Gernesis energy dispersive

spectrometer (EDAX, USA). Raman spectra was recorded on a LabRam HR800 Raman spectrometer (Horiba Jobin Yvon, France) by a 633 nm laser source. X-ray diffraction (XRD) pattern was performed on a D8 Advance X-ray diffractometer (Bruker, Germany) with a Cu K α radiation source ($\lambda = 1.54056$ Å). X-ray photoelectron spectroscopy (XPS) measurements were performed by a Thermo Scientific Escalab 250Xi X-ray photoelectron spectrometer (Thermo Fisher Scientific, USA). All the electrochemical measurements such as CV, DPV and electrochemical impedance spectroscopy (EIS) were performed on a CHI660D electrochemical work station (Shanghai Chenhua Instrument Co. Ltd., China). A conventional three-electrode system was used for all electrochemical experiments system, which consisted of a modified glassy carbon electrode (GCE) as the working electrode (diameter of 3.0 mm), a saturated calomel electrode (SCE) as the reference electrode and a platinum wire (diameter of 1.0 mm) as the counter electrode. All the pH values of BR buffer solutions were measured with a CT-6023 pH meter (Shenzhen Ke Dida Electronics Co., Ltd., China).

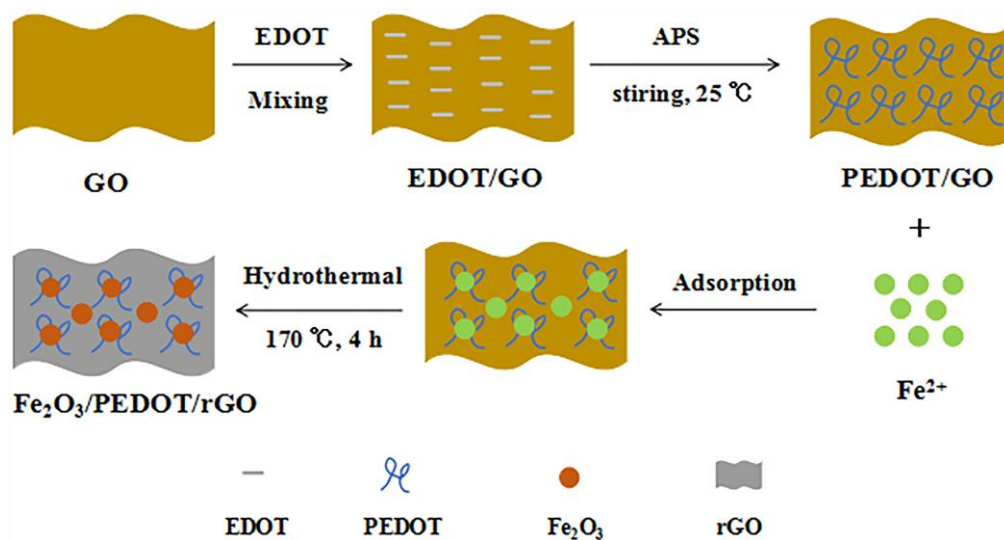
2.2 Chemicals and reagents

Graphite (GR) powders and ammonium peroxodisulfate (APS) were purchased from Shanghai Vita Chemical Reagent Co., Ltd. China. 3,4-Ethylenedioxythiophene (EDOT) monomer was bought from Energy Chemical (Shanghai, China) and purified by distilled under reduced pressure before use. Caffeine was bought from Chemservice Co. Ltd. Iron(II) chloride, ammonia and the other reagents were purchased from Aladdin Chemistry Co., Ltd. All these reagents were analytical grade and used without further purification. All the solutions were prepared by the deionized water.

2.3 Synthesis of Fe₂O₃/PEDOT/rGO nanocomposite

Graphene oxide (GO) was prepared from graphite powders with the modified Hummers method [22]. The ternary Fe₂O₃/PEDOT/rGO nanocomposite was synthesized by one-pot method. Firstly, 20 mg GO was dispersed in 40 mL deionized water and ultrasonicated for 30 min. Then, 0.25 mL EDOT dissolved in 5 mL ethanol was added into previous GO aqueous dispersion drop by drop. Subsequently, 5 mL APS aqueous solution (0.05 g mL⁻¹) was slowly poured into the mixture with stirring. After 12 h of stirring under the room temperature, the mixture turned into dark blue, most of the EDOT had been turned into PEDOT. Afterwards, 200 μ L 25% ammonia and different amounts of FeCl₂ (0.02 g, 0.04 g, 0.06 g, 0.1 g, 0.2 g) were added into the mixture solution in order to explore the best additive quantity of FeCl₂. Subsequently, the mixture was poured into a Teflonlined stainless steel autoclave, and the autoclave was maintained at 170 °C for 4 h, then cooled to room temperature by cold water. Finally, the obtained mixture was centrifuged and washed with ethanol and deionized water for three times each, and dried at 60 °C for 12 h in a vacuum oven (Scheme 1). For comparison, Fe₂O₃/rGO were prepared by previously reported method [18]. The main experimental process is as follows: Similarly, 20 mg GO was dispersed in 40 mL deionized water, ultrasonicated for 30 min. Then, 200 μ L 25% ammonia and 0.04 g FeCl₂ were added into the GO dispersion under stirring,

respectively. Subsequently, the mixture was poured into a Teflonlined stainless steel autoclave, and maintained at 170 °C for 4 h. Finally, the obtained mixture was processed with washing and drying.



Scheme 1. Schematic illustration for the preparation of $\text{Fe}_2\text{O}_3/\text{PEDOT}/\text{rGO}$ composite

2.4 Optimization of the amounts of FeCl_2

In order to find out the optimal amount of Fe^{2+} , five different amounts of FeCl_2 (0.02 g, 0.04 g, 0.06 g, 0.1 g, 0.2 g) were used in the preparation of $\text{Fe}_2\text{O}_3/\text{PEDOT}/\text{rGO}$ composites. The CV curves of the five different prepared $\text{Fe}_2\text{O}_3/\text{PEDOT}/\text{rGO}$ composites in BR buffer solution (pH = 1.8) with 0.1 mM caffeine were obtained accordingly. As a result, when added 0.04 g FeCl_2 , we get the highest peak current. Therefore, 0.04 g FeCl_2 was settled for the preparation of $\text{Fe}_2\text{O}_3/\text{PEDOT}/\text{rGO}$ in the subsequent experiments.

2.5 Preparation of modified electrode

Firstly, the glassy carbon electrodes were polished repeatedly with 0.5 μm alumina slurries, and then sonically washed in deionized water and ethanol, each for 3 min. After that, 5 μL of $\text{Fe}_2\text{O}_3/\text{PEDOT}/\text{rGO}$ suspensions (dispersed in water, 1 mg mL^{-1}) were applied on the surface of the GCE and dried at room temperature. For comparison, $\text{Fe}_2\text{O}_3/\text{rGO}$ modified GCE were prepared under the same conditions.

3. RESULTS AND DISCUSSION

3.1 Characterization of $\text{Fe}_2\text{O}_3/\text{PEDOT}/\text{rGO}$ nanocomposite

The morphology of $\text{Fe}_2\text{O}_3/\text{PEDOT}/\text{rGO}$ nanocomposite was characterized by SEM (Fig. 1b). For comparison, the $\text{Fe}_2\text{O}_3/\text{rGO}$ nanocomposite was also characterized by SEM (Fig. 1a). As shown in Fig. 1a, Fe_2O_3 nanoparticles are attached to the surface of the rGO tightly, and most of the

nanoparticles gather together to become nanoclusters eventually. Fig. 1b shows the micrographs of $\text{Fe}_2\text{O}_3/\text{PEDOT}/\text{rGO}$ nanocomposites, it can be seen that Fe_2O_3 nanoparticles have larger specific surface area, and the whole composites become irregular, fluffy and wrinkled owing to the introduction of PEDOT.

Energy dispersive spectrum (EDS) analysis was used to confirm the components of the $\text{Fe}_2\text{O}_3/\text{PEDOT}/\text{rGO}$ nanocomposites. As shown in Fig. 1c, element S comes from the PEDOT, element Fe comes from Fe_2O_3 . The content of each element was listed in the inset table.

To explore the structure characteristics of carbon-based materials, Raman spectroscopy is the most frequently technique [23]. Fig. 1d shows the Raman spectrum of $\text{Fe}_2\text{O}_3/\text{PEDOT}/\text{rGO}$. The important Raman features in the Fe_2O_3 can be observed in two classes of Raman active vibration modes, A_{1g} modes ($215, 504 \text{ cm}^{-1}$) and E_g modes ($280, 407, 604 \text{ cm}^{-1}$) [24]. The two strong absorption at 1425 and 1488 cm^{-1} are attributed to a $C_\alpha=C_\beta$ symmetric stretching vibration and asymmetrical stretching vibration in the PEDOT [25]. Furthermore, the Raman features in the rGO can be observed at 1363 cm^{-1} (D band) and 1600 cm^{-1} (G band) [26].

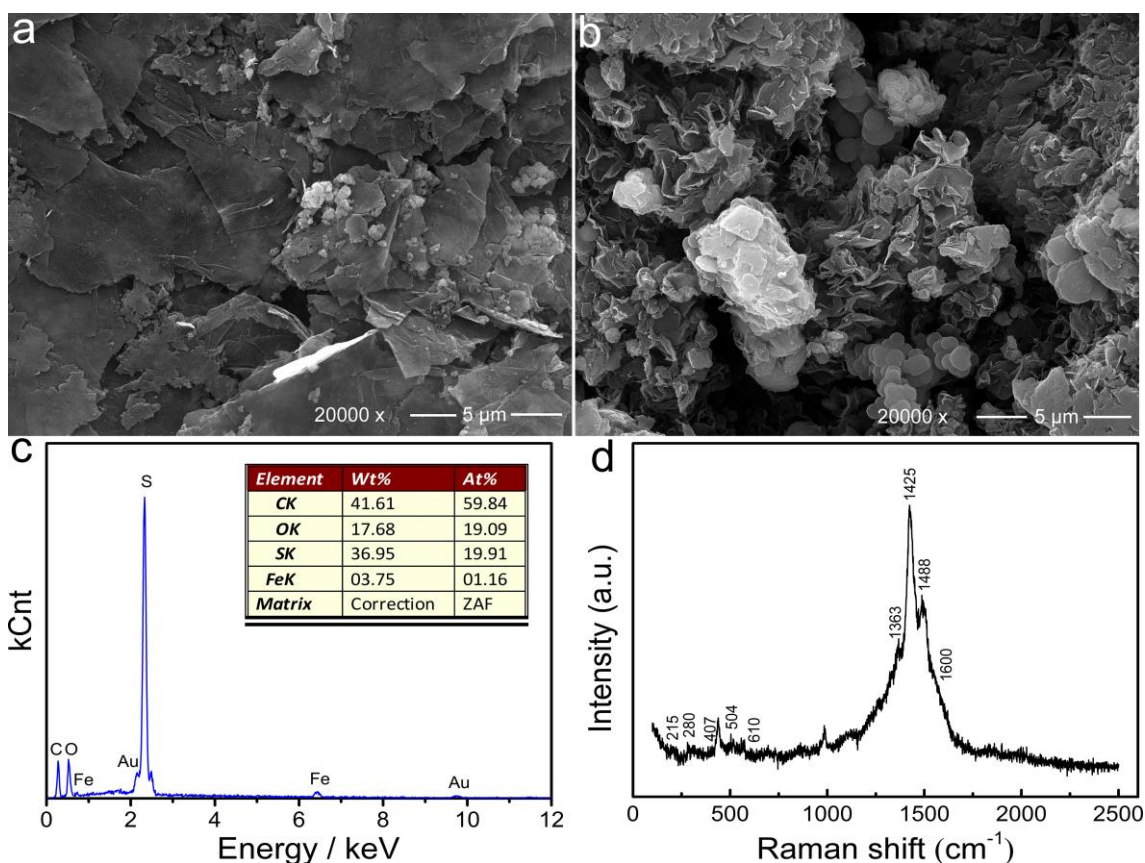


Figure 1. SEM images of $\text{Fe}_2\text{O}_3/\text{rGO}$ (a) and $\text{Fe}_2\text{O}_3/\text{PEDOT}/\text{rGO}$ (b); the EDS (c) and Raman spectra (d) of $\text{Fe}_2\text{O}_3/\text{PEDOT}/\text{rGO}$.

Furthermore, the nanocomposite was characterized by XRD and XPS. Fig. 2a shows the XRD pattern of $\text{Fe}_2\text{O}_3/\text{PEDOT}/\text{rGO}$. The peaks are centered at $23.9^\circ, 33^\circ, 35.4^\circ, 40.7^\circ, 49.3^\circ, 53.9^\circ, 57.4^\circ,$

62.3° and 63.9°, where all the peaks exhibits the crystalline Fe₂O₃ diffraction peaks, verifying the existence of α -Fe₂O₃ [27].

Fig. 2b shows the XPS spectrum of Fe₂O₃/PEDOT/rGO. These peaks in the wide-scan XPS spectrum correspond to the characteristic peaks of C1s, O1s, S2p, Fe2p and Fe3p. This result is consistent with previous EDS analysis in Fig. 1c. Moreover, Fig. 2c and d show the XPS spectra of Fe2p and S2p respectively. Fig. 2c exhibits two major peaks at 711.2 and 724.9 eV, corresponding to Fe2p_{3/2} and Fe2p_{1/2}, respectively, which is characteristic of Fe³⁺ in Fe₂O₃ [28]. And in the Fig. 2d, the two peaks at 162.9 and 163.8 eV are corresponding to S2p_{3/2} and S2p_{1/2}, respectively [29]. According to the results of different characterizations, we can confirm that Fe₂O₃/PEDOT/rGO nanocomposite is obtained successfully by the one-pot method.

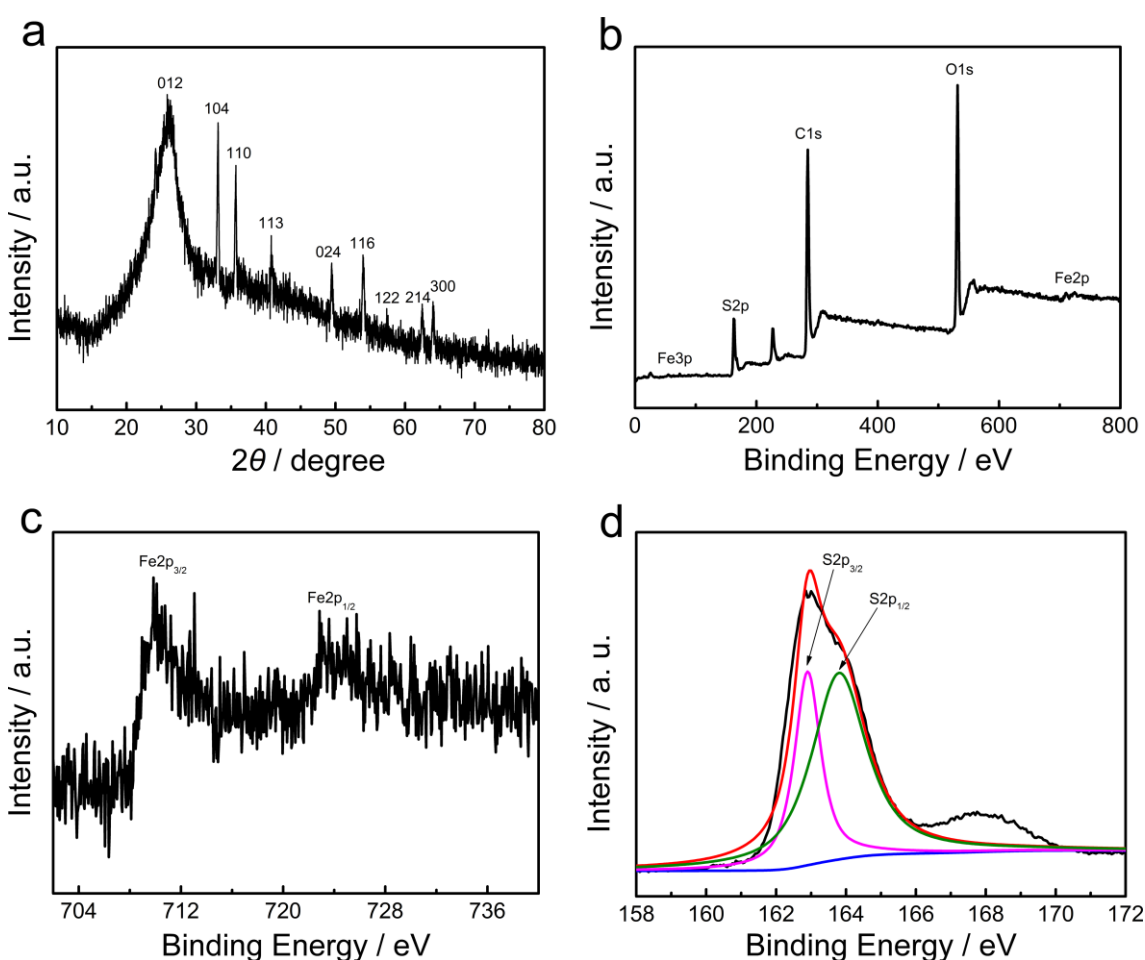


Figure 2. XRD patterns (a) and XPS survey spectra (b) of Fe₂O₃/PEDOT/rGO; High resolution Fe2p (c) and S2p (d) XPS spectra of Fe₂O₃/PEDOT/rGO.

3.2 Electrochemical characterization of the Fe₂O₃/PEDOT/rGO/GCE

The CV curves of the bare GCE, Fe₂O₃/rGO/GCE, Fe₂O₃/PEDOT/rGO/GCE were recorded in the presence of 5.0 mM K₃Fe(CN)₆/K₄Fe(CN)₆ (1:1) containing 0.1 M KCl at a scan rate of 50 mV s⁻¹ (Fig. 3a). We can observe good redox peaks at the three electrodes. However, the peak current of the

modified electrode was obviously higher than that at bare GCE, and the peak current of $\text{Fe}_2\text{O}_3/\text{PEDOT}/\text{rGO}/\text{GCE}$ was higher than $\text{Fe}_2\text{O}_3/\text{rGO}/\text{GCE}$, indicating that $\text{Fe}_2\text{O}_3/\text{rGO}$ and PEDOT all increased the value of the response current by enlarging the effective surface area and electrical conductivity. Moreover, Fig. 3b shows the representative EIS spectra of the three electrode. As shown in the EIS spectra, the bare GCE had a large resistance. When $\text{Fe}_2\text{O}_3/\text{rGO}$ or $\text{Fe}_2\text{O}_3/\text{PEDOT}/\text{rGO}$ nanocomposite was modified on the GCE, a remarkable decrease in the Ret value was observed, and the Ret value in $\text{Fe}_2\text{O}_3/\text{PEDOT}/\text{rGO}$ decreased more, which indicated the superior electrochemical activity and conductivity of $\text{Fe}_2\text{O}_3/\text{PEDOT}/\text{rGO}$ nanocomposite.

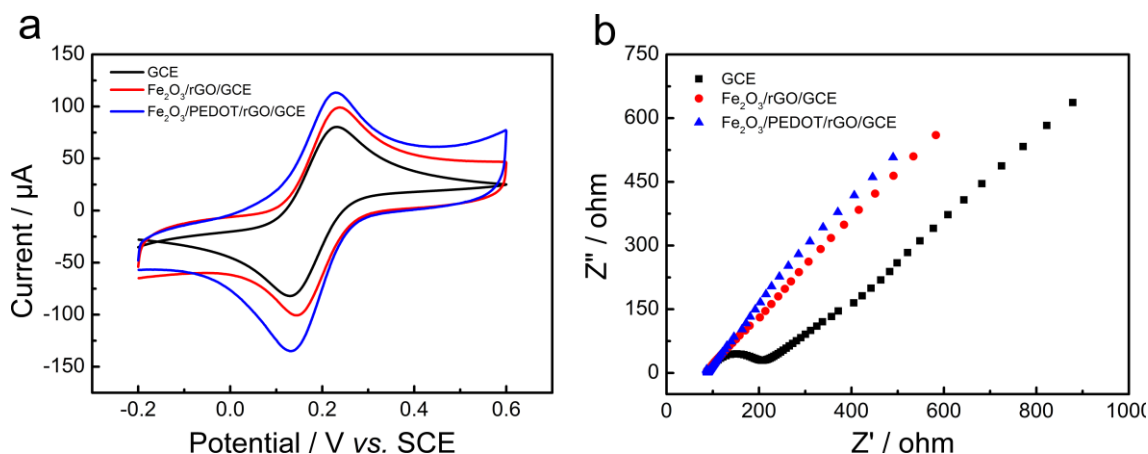


Figure 3. CVs (a) and the representative impedance spectrum (b) of the bare GCE, $\text{Fe}_2\text{O}_3/\text{rGO}/\text{GCE}$, and $\text{Fe}_2\text{O}_3/\text{PEDOT}/\text{rGO}/\text{GCE}$ in 5.0 mM $\text{K}_3\text{Fe}(\text{CN})_6/\text{K}_4\text{Fe}(\text{CN})_6$ (1:1) containing 0.1 M KCl.

3.3 Electrochemical behavior of caffeine at the $\text{Fe}_2\text{O}_3/\text{PEDOT}/\text{rGO}/\text{GCE}$

Fig. 4 shows the cyclic voltammogram responses and anodic peak current response of the $\text{Fe}_2\text{O}_3/\text{PEDOT}/\text{rGO}/\text{GCE}$ with 0.1 mM caffeine and different pH values (1.8, 2.0, 2.5, 3.0, 3.5) of BR buffer solutions. It can be seen that the peak current had been decreasing with pH in the range of 1.8–3.5. Therefore, the BR buffer solutions (pH = 1.8) was selected as the supporting electrolyte in following experiments.

Fig. 5a shows the cyclic voltammogram responses at bare GCE, $\text{Fe}_2\text{O}_3/\text{rGO}/\text{GCE}$ and $\text{Fe}_2\text{O}_3/\text{PEDOT}/\text{rGO}/\text{GCE}$ in the presence of 0.1 mM caffeine in BR buffer solution (pH = 1.8). As we can see, there is a big and sharp oxidation peak at 1.35 V on the CV curve of $\text{Fe}_2\text{O}_3/\text{PEDOT}/\text{rGO}/\text{GCE}$, which was corresponding to the oxidation process of caffeine [30]. Furthermore, there is no peak observed on the CV of $\text{Fe}_2\text{O}_3/\text{PEDOT}/\text{rGO}/\text{GCE}$ without caffeine. By comparison with the CVs on the bare GCE and $\text{Fe}_2\text{O}_3/\text{rGO}/\text{GCE}$, the CV on $\text{Fe}_2\text{O}_3/\text{PEDOT}/\text{rGO}/\text{GCE}$ shows the highest oxidation peak current, demonstrating the excellent electrocatalytic activity toward the oxidation of caffeine.

As shown in Fig. 5b, with the increase of scan rates, the anodic peak current clearly increased. The anodic current was linearly correlation with the square root of scan rate in the range of 50–400 mV s^{-1} , and the linear regression equation was $I_{\text{pa}} (\mu\text{A}) = 0.796 v^{1/2} (\text{mV}^{1/2} \text{s}^{-1/2}) + 5.309$ ($R = 0.995$), which indicated that the electrode reaction was controlled by diffusion process.

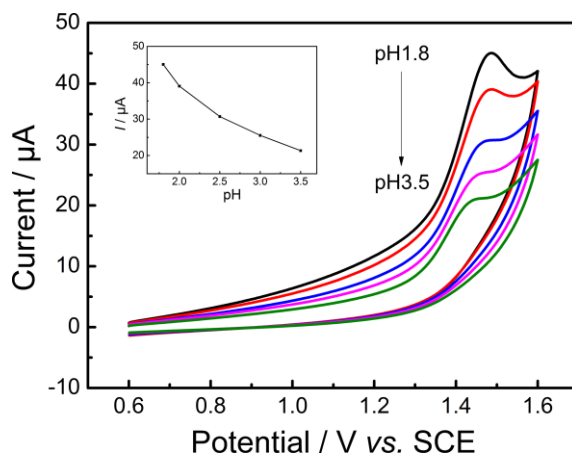


Figure 4. CVs of the Fe₂O₃/PEDOT/rGO/GCE in different BR buffer solutions (pH = 1.8, 2.0, 2.5, 3.0, 3.5) with 0.1 mM caffeine, scan rate: 50 mV s⁻¹.

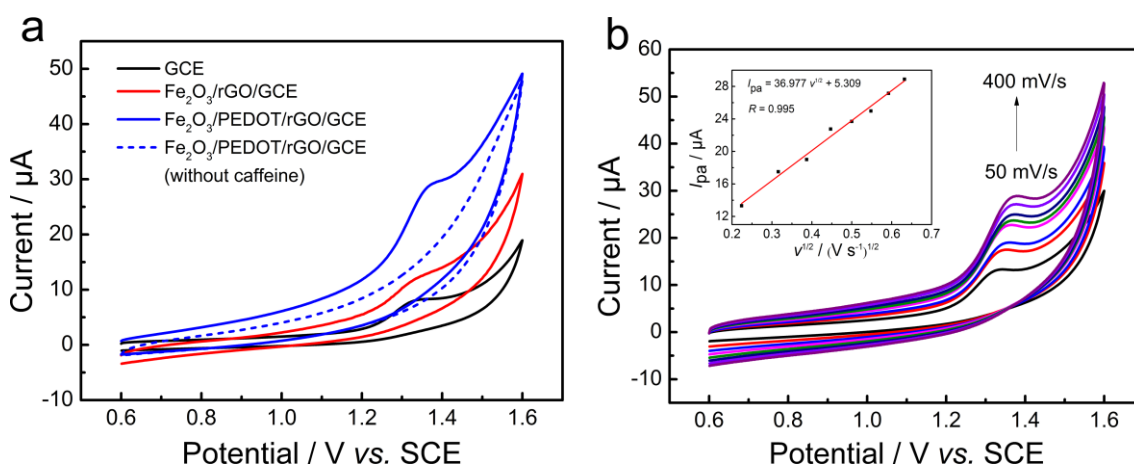


Figure 5. CVs (a) at bare GCE, Fe₂O₃/rGO/GCE, and Fe₂O₃/PEDOT/rGO/GCE in the presence of 0.1 mM caffeine and Fe₂O₃/PEDOT/rGO/GCE in the absence of caffeine in BR buffer solution (pH = 1.8), scan rate: 50 mV s⁻¹; CVs (b) of Fe₂O₃/PEDOT/rGO/GCE in the presence of 0.1 mM caffeine in BR buffer solution (pH = 1.8) at different scan rates (50–400 mV s⁻¹). Inset: plots of peak current vs. the square root of scan rate ($v^{1/2}$).

3.4 Differential pulse voltammetry detection of caffeine at the Fe₂O₃/PEDOT/rGO/GCE

Fig. 6a shows the DPV curves of the Fe₂O₃/PEDOT/rGO/GCE in different concentrations of caffeine from 1 to 800 µM. When the concentration changed from 1.0×10^{-6} M to 8.0×10^{-4} M, the anodic peak current of caffeine was linearly related to the concentration over the range of 1.0×10^{-6} – 1.0×10^{-4} M and 1.0×10^{-4} – 8.0×10^{-4} M, respectively (Fig. 6b). The linear regression equations were $I_{pa} = 0.045 C + 1.748$ ($R^2 = 0.992$) for the range of 1.0×10^{-6} – 1.0×10^{-4} M and $I_{pa} = 0.025 C + 4.246$ ($R^2 = 0.992$) for the range of 1.0×10^{-4} – 8.0×10^{-4} M, and the detection limit was calculated to be 0.33 µM (S/N = 3).

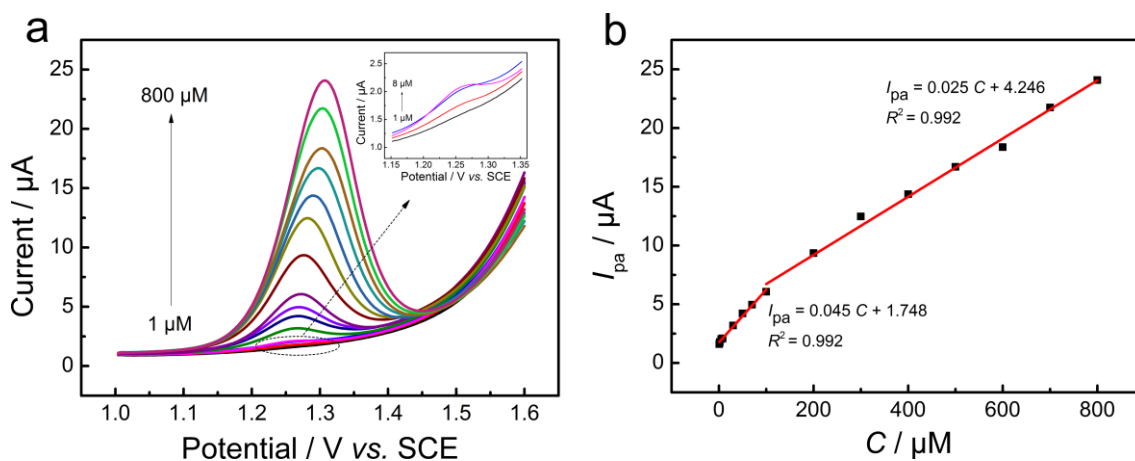


Figure 6. DPVs (a) of the $\text{Fe}_2\text{O}_3/\text{PEDOT}/\text{rGO}$ obtained in the BR buffer solution (pH=1.8) containing different concentrations of caffeine; The linear relationship (b) between the oxidation peak current and concentration of caffeine in the range of 1×10^{-6} M to 8×10^{-4} M.

Table 1 listed the analytical performances of $\text{Fe}_2\text{O}_3/\text{PEDOT}/\text{rGO}/\text{GCE}$ and other modified electrodes reported in the literature for the determination of caffeine. Compared with most of the modified electrodes, the $\text{Fe}_2\text{O}_3/\text{PEDOT}/\text{rGO}/\text{GCE}$ showed better detection limit and detection range.

Table 1. Comparison of the electrochemical sensing performance of different modified electrodes toward caffeine detection.

Modified electrode	Technique	Linear rang (μM)	Detection limit (μM)	References
BDDE	DPV	9.7-110	7.0	[30]
PT/TiO ₂ -GR/GCE	DPV	25-200	0.5	[31]
Nafion/GCE	DPV	0.995-10.6	0.79	[32]
CeHCF/GO/GCE	DPV	1-130	0.52	[33]
DNA-CNTs/CPE	DPV	0.512-61.7	0.35	[34]
MWNTs-Nafion/GCE	DPV	2.945-377.0	0.513	[35]
$\text{Fe}_2\text{O}_3/\text{PEDOT}/\text{rGO}/\text{GCE}$	DPV	1-800	0.33	This work

3.5 Reproducibility, stability and selectivity of $\text{Fe}_2\text{O}_3/\text{PEDOT}/\text{rGO}/\text{GCE}$

The reproducibility of the modified electrode was studied by following method. For five successive determinations in the presence of 0.1 mM caffeine with a single modified electrode, the relative standard deviation (RSD) of the peak currents was 3.4%. Moreover, a series of five modified

electrodes were prepared by the same way, and the relative standard deviation was 4.6%. As a result, the proposed method had an excellent reproducibility for caffeine determination. In addition, the stability of the prepared sensor was investigated. After being stored in a refrigerator (4 °C) for 30 days, the sensor retained 90% of its original response, which showed good long-term stability.

Possible interferences for the detection of caffeine at the Fe₂O₃/PEDOT/rGO/GCE were investigated by adding various foreign species into the BR buffer solution (pH = 1.8) containing 0.1 mM caffeine. A relative error of 5% was considered tolerable. The results indicated that common ions, such as K⁺, Na⁺, Mg²⁺, Fe³⁺, Zn²⁺, Cu²⁺, NO₃⁻, SO₄²⁻, Cl⁻, and CO₃²⁻ in a 100-fold concentration and glucose, D-Fructose, Caffeic acid, Citric acid, Ascorbic acid, L-Glutamic acid in the same concentration had no influence in the detection of caffeine, which demonstrated the good selectivity about the proposed method.

3.6 Real sample analysis

In order to evaluate the applicability of Fe₂O₃/PEDOT/rGO/GCE in real samples, the prepared sensor was used to detect caffeine in energy beverages. For the reliability of test, the standard addition method was used to determine the diluted energy beverage sample spiked with suitable caffeine, the results were listed in Table 2. The recoveries were in the range of 99.93% to 102.41%, which proved the high accuracy of the proposed method.

Table 2. Determination of caffeine in energy beverage sample (*n*=5)

Added (μM)	Detected (μM)	Recovery (%)	RSD (%)
0	26.48	–	1.25
20	46.69	100.45	3.62
40	68.08	102.41	2.74
60	86.42	99.93	2.76

4. CONCLUSION

In summary, a novel ternary nanocomposite was fabricated via one-pot method, and a new electrochemical sensor based on Fe₂O₃/PEDOT/rGO/GCE for the sensitive determination of caffeine was developed. The experimental data showed that the prepared sensor had a good electrocatalytic activity towards the oxidation of caffeine, and it was stable and repeatable in detecting caffeine. Moreover, the developed method was applied to analysis caffeine in beverage samples successfully.

ACKNOWLEDGEMENTS

The financial supports from the National Natural Science Foundation of China (51463008 and 51502118), the Provincial Natural Science Foundation of Jiangxi (20161BAB216131), and the Dr Startup fund of Jiangxi Science and Technology Normal University (3000990315) are sincerely appreciated by the authors.

References

1. A. Nehlig, J.L. Daval and Debry G, *Brain Res. Rev.*, 17 (1992) 139.
2. H. Ashihara and T. Suzuki, *Front. Biosci.*, 9 (2004) 1864.
3. C.D. Frary, R.K. Johnson and M. Wang, *J. Am. Diet. Assoc.*, 105 (2005) 110.
4. R. Blecher, F. Lingens and Z. Hoppe-Seyler's, *Physiol. Chem.*, 358 (1977) 807.
5. S. Ahmad, A. Khalid, N. Parveen, A. Babar, R.A. Lodhi, B. Rameez, A. Shafi, N. Noor and F. Naseer, *Bull. Env. Pharmacol. Life Sci.*, 5 (2016) 15.
6. M. Palo, K. Kogermann, N. Geninaa, D. Fors, J. Peltonen, J. Heinämäki and N. Sandler, *J. Drug Deliv. Sci.Tec.*, 34(2016) 60.
7. P. Pokhrel, S. Shrestha, S.K. Rijal and K.P. Rai, *Int. J. Food Sci.Tech.*, 9 (2016) 74.
8. W.F. Zhang, Y.H. Zhang, L.L. Zhou, S.N. Zhao, H.F. Du, X. Ma and S.S. Zhang, *Anal. Methods*, 8 (2016) 3613.
9. J.G. Lisko, G.E. Lee, J.B. Kimbrell, M.E. Rybak, L. Valentin-Blasini and C.H. Watson, *Nicotine Tob. Res.*, 19 (2017) 484.
10. M.C. Marra, P.L. Silva, R.A. Muñoz and E.M. Richter, *J. Braz. Chem. Soc.*, 25 (2014) 913.
11. A.K. Sundramoorthy, O. Sadak, S. Anandhakumar and S. Gunasekarana, *J. Electrochem. Soc.*, 163 (2016) 638.
12. Y.X. Liu, X.C. Dong and P. Chen, *Chem. Soc. Rev.*, 41 (2012) 2283.
13. J.Y. Sun, K.J. Huang, S.Y. Wei, Z.W. Wu and F.P. Ren, *Colloid Surface B*, 84 (2011) 421.
14. F.Y. Zhao, F. Wang, W.N. Zhao, J. Zhou, Y. Liu, L.N. Zou and B.X. Ye, *Microchim. Acta*, 174 (2011) 383.
15. L. Svorc, *Int. J. Electrochem. Sci.*, 8 (2013) 5755.
16. Y. Qian, F.C. Ye, J.P. Xu and Z.G. Le, *Int. J. Electrochem. Sci.*, 7 (2012) 10063.
17. S.J. Prabakar, Y.H. Hwang, E.G. Bae, S. Shim, D. Kim, M.S. Lah, K.S. Sohn and M. Pyo, *Adv. Mater.*, 25 (2013) 3307.
18. S. Radhakrishnan, K. Krishnamoorthy, C. Sekar, J. Wilson and S.J. Kim, *Appl. Catal. B-Enviro.*, 148 (2014) 22.
19. R.R. Yue, H.W. Wang, D. Bin, J.K. Xu, Y.K. Du, W.S. Lu and J. Guo, *J. Mater. Chem. A*, 3 (2015) 1077.
20. W.J. Wang, W. Lei, T.Y. Yao, X.F. Xia, W.J. Huang, Q.L. Hao and X. Wang, *Electrochim. Acta*, 108 (2013) 118.
21. J.E. Choe, J.M. You, M. Yun, K. Lee, M.S. Ahmed, Z. Ustundag and S. Jeon, *J. Nanosci. Nanotechno.*, 15 (2015) 5684.
22. W.S. Hummers and R.E. Offeman, *J. Am. Chem. Soc.*, 80 (1958) 1339.
23. L.M. Malard, M.A. Pimenta, G. Dresselhaus and M.S. Dresselhaus, *Phys. Rep.*, 473 (2009) 51.
24. W. Wu, R. Hao, F. Liu, X.T. Su and Y.L. Hou, *J. Mater. Chem. A*, 1 (2013) 6888.
25. S.Y. Wang, L.P. Zhang, Z.H. Xia, A. Roy, D.W. Chang, J.B. Baek and L.M. Dai, *Angew. Chem. Int. Edit.*, 51 (2012) 4209.
26. P.B. Liu, Y. Huang and X. Zhang, *Powder Technol.*, 276 (2015) 112.
27. Z.G. An, J.J. Zhang, S.L. Pan and F. Yu, *J. Phys. Chem. C*, 113 (2009) 8092.
28. X.J. Liu, J.F. Liu, Z. Chang, L. Luo, X.D. Lei and X.M. Sun, *RSC Adv.*, 3 (2013) 8489.
29. S.A. Spanninga, D.C. Martin and Z. Chen, *J. Phys. Chem. C*, 113 (2009) 5585.

30. B.H. Hansen and G. Dryhurst, *J. Electroanal. Chem. Interf. Electrochem.*, 30 (1971) 407.
31. X.Q. Xiong, K.J. Huang, C.X. Xu, C.X. Jin and Q.G. Zhai, *Chem. Ind. Chem. Eng. Q.*, 19 (2013) 359.
32. B. Brunetti, E. Desimoni and P. Casati, *Electroanal.*, 19 (2007) 385.
33. X.C. Lu, K.J. Huang, Z.W. Wu, S.F. Huang and C.X. Xu, *Chinese J. Anal. Chem.*, 3 (2012) 452.
34. S.Y. Ly, C.H. Lee and Y.S. Jung, *NeuroMol. Med.*, 11 (2009) 20.
35. J. Zhang, L.P. Wang, W. Guo, X.D. Peng, M. Li and Z.B. Yuan, *Int. J. Electrochem. Sci.*, 6 (2011) 997.

© 2018 The Authors. Published by ESG (www.electrochemsci.org). This article is an open access article distributed under the terms and conditions of the Creative Commons Attribution license (<http://creativecommons.org/licenses/by/4.0/>).